Faculty of Materials and Chemical Engineering
University of Miskolc
ANTAL KERPELY DOCTORAL SCHOOL OF
MATERIALS SCIENCE & TECHNOLOGY
Head of Doctoral School
Prof. Dr. Valéria Mertinger

Thesis Booklet of the Doctoral Dissertation

entitled

Molecular Dynamics Aided Green Transition of Selected Problems in the Chemical Industry

Molecular-level understanding of membrane permeation of some chemicals and the phase diagram of 1,3-butadiene.

Zsófia Borbála Rózsa

Supervisor

Prof. Dr. Milán Szőri

Institute of Chemistry
University of Miskolc

Miskolc, Hungary

2022

INTRODUCTION

To this day, over 350 000 chemicals and mixtures of chemicals are registered for production and use [1], which annual production rate exceeds 10^8 tons. [2] While chemicals are essential to our life standards, a non-negligible portion of the produced substances is released into the environment due to improper handling during their production, usage and disposal. Environmental exposure is a key contributor to diseases, premature death and the alteration of ecosystems, chemical pollution is also considered as one of the major factor in climate change and responsible for disintegration of the biosphere. [3]

It is clear that the physicochemical properties of the present chemicals are multifarious, thus it is necessary to label, classify and predict their mode of toxic action (MOA) in order to understand their toxicological properties for accurate environmental risk assessment. [4] As the majority of industrial chemicals were not designed to interfere with biological activities, aside from reactive chemicals, industrial compounds generally lack the structural attributes to initiate specific toxic pathways. Even if these chemicals cannot bind selectively to biological receptors, they are able to interact with biological membranes through weaker and reversible hydroapatic interactions. [5], [6] The MOA of these chemicals is via narcosis, which is the non-specific toxic action on the cell membranes, leading to the reversible disruption of its functions. While it is clear, that narcotic chemicals accumulate within biological membranes, the exact cause of toxicity is still undefined. [7] According to Mullins if the volume fraction (V/V) of a narcotic compound in the membrane is higher than 0.003, narcosis will occur. [8] For the support of environmental and toxicological sciences, less-known, chemically inert industrial compounds can be characterized while their hydroapatic partitioning can be inspected, all by using the modern tools of computational chemistry. [9], [10]

Aromatic hydrocarbons are present in several classical industrial processes. The family of these molecules is diverse and includes species such as the nitrogen, sulfur or oxygen containing heterocyclic hydrocarbons (NSO-HETs). Due the lipophilic nature of NSO-HETs the primary site of their toxicity is the cell membrane. Accumulation of compounds in the membrane may lead to the alteration of the membrane structure and function, which can lead to the penetration of additional molecules. [11], [12] At the same time several NSO-HETs are suspected or proven to be embryotoxic [13] or carcinogenic. [14] While 1,4-dioxane, morpholine, oxane and phenol are industrially already applied NSO-HET molecules, their behavior in the vicinity of biomembranes, the kinetics of their penetration and their membrane altering effects are yet to be understood.

The telomerisation reaction of CO_2 and 1,3-butadiene results in the synthesis of a highly functionalized δ-lactone, 3-ethylidene-6-vinyltetrahydro-2H-pyran-2-one (EVL) which is a promising monomer for the production of synthetic ‘green’ polymers. Efforts have been made to improve the conversion rate and selectivity of the reaction for EVL formation. At the same time about a 14% yield of side products appear during

the reaction, such as a covalent butadiene dimer (octa-1,3,7-triene, BDDI), acids (2-vinylhepta-4,6-dienoic acid, AC1 and 2-ethylhepta-4,6-dienoic acid, AC2) and other lactones composed of five membered heterocycles (3-ethylidene-2-methylene-5-(prop-1-en-1-yl)-dihydrofuran, LAC2; 3-ethyl-5-propylidenefuran-2-on, LAC3). [15]–[17] Aside from the known reaction of 1,3-butadiene and CO_2, there is a lack of information in previous studies on the products, either their pure liquid properties or their environmental effects.

Physicochemical properties of supercritical fluids (SCFs) such as density, diffusivity, viscosity and dielectric constant can be modified on a large scale by changing the pressure and/or temperature, therefore SCFs can be used broadly as reaction media and their application can also allow selective and faster extraction in separation processes. These features make SCFs an attractive alternative to liquid solvents, while collecting experimental data from these extreme conditions can be challenging due to the increased hazards and the need of specialized equipment, where a wide range of variables are needed to be investigated. [18]–[20] To further optimize the latter reaction, 1,3-butadiene was investigated structurally and thermochemically from the VLE to the supercritical phase by the means of classical molecular dynamics simulations.

MOTIVATION OF THIS THESIS

Due to this day, several xenobiotics are emitted into the environment without proper handling and understanding the dangers they can pose to biological entities. The motivation of my work was to better understand the effect of potential environmental pollutants on biological membranes, and to promote the development of greener technologies by using molecular dynamics simulations. Even if using the means of MD for these problems is still in the early stage, understanding molecular processes can be of great help to broaden the knowledge on pollution pathways, classify chemicals based on their membrane altering effects and to help in setting up environmental risk assessments. At the same time modern computational methods also provide atomistic level of understanding of hardly accessible chemical states. By using these information, chemical processes can be optimized for higher selectivity or lower solvent usage, in order to reduce the amount of unwanted side products and prevent the production of further environmental pollutants.

In my thesis I am introducing the results I have obtained by investigating the effects of 10 industrial, potential environmental pollutant molecules on model biomembranes, shown on **Figure 1** [21]–[23] At the same time I am also showing the results I have obtained for the structural changes of 1,3-butadiene from the VLE to the supercritical conditions [24] which could further help in understanding and optimizing the production of EVL, a potential 'green' monomer for polymer synthesis.

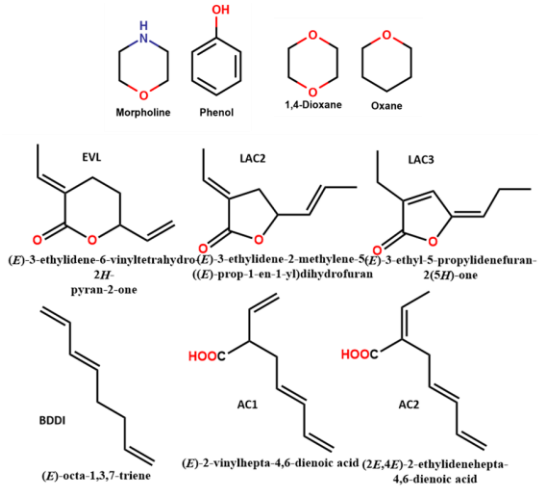

Figure 1 2D representation of the potential environmental pollutants investigated in my studies. The simplified names of the molecules indicated next to the structures are used throughout this study.

METHODS

CLASSICAL MOLECULAR DYNAMICS

Molecular simulations based on detailed atomistic models and realistic microscopic interactions represent a powerful tool to gain insight into the structure and dynamics of complex molecular systems and to understand the microscopic origin of a given phenomena. Molecular Dynamics (MD) simulations solve the Newtonian equations of motion over an ensemble of molecules to predict their coordinates at different time steps, then calculates the potential energy of the system by using force fields. Force fields are mathematical expressions describing the dependence of the systems' potential energy on the coordinates of its particles. The potential energy can be obtained by the summation of the intra- and intermolecular interactions affecting each atom:

$$E_{\text{pot}} = E_{\text{str}} + E_{\text{angles}} + E_{\text{torsion}} + E_{\text{vdW}} + E_{\text{ele}} \qquad Eq.1$$

, where the first four terms refer to intramolecular contributions to the total energy (E_{str}: bond stretching, E_{angles}: angle bending and E_{torsion}: dihedral), and the last two terms refer to the van der Waals (E_{vdW}) and Coulombic (E_{ele}) interactions. [25]

FREE ENERGY OF PERMEATION

Gibbs free energy (G), is the maximum amount of work a system can do at a constant pressure and temperature. The change in G in a molecular system can be obtained by the following equation, where ΔU is the change in potential energy, T is the temperature, ΔS is the change in entropy, P is pressure and ΔV is the volume change: [26]

$$\Delta G = \Delta U - T\Delta S + P\Delta V \qquad Eq.2$$

To transform a molecular system from one thermodynamic state to another, free energy is needed. To estimate the difference in free energy (ΔG_{BA}) between configurations A and B of the same system, one has to estimate the ratio of partition functions (Q) between them. [27]

$$\Delta G_{BA} = G_B - G_A = -k_B T \ln \frac{Q_{NPT,B}}{Q_{NPT,A}} \qquad Eq.3$$

If one well defined chemical, mechanical or thermodynamic process needs to be analyzed, it can frequently be represented by a set of low dimensional, generalized coordinates. These coordinates are usually called collective variables (CV). A CV is a function of the atomic coordinates that is capable of describing the physics behind the process under investigation. [28] The probability density distribution (ρ) of the CV at

state A and state B ($\rho(\mathrm{CV(s)}_A)$ and $\rho(\mathrm{CV(s)}_B)$ respectively) can be calculated from the ratio of partition function of states A and B:

$$\frac{\rho(\mathrm{CV(s)_B})}{\rho(\mathrm{CV(s)}_A)} = \frac{\mathrm{Q}_{NPT,B}}{\mathrm{Q}_{NPT,A}} \qquad Eq.4$$

Therefore, the free energy difference between states A and B can be obtained as the ratio of the probability of the different states, where k_B is the Boltzmann constant:

$$\Delta G_{BA} = -k_B T \ln \frac{\rho(\mathrm{CV(s)}_B)}{\rho(\mathrm{CV(s)}_A)}. \qquad Eq.5$$

As the free energy is directly related to the probability of the states along a chosen collective variable (CV(s)), the free energy landscape the process ($G(s)$) can be directly obtained from the probability density distribution of the configurations along s [29]:

$$G(s) = -k_B T \ \ln\langle\rho(s)\rangle \qquad Eq.6$$

A computationally inexpensive approach for calculating the free energy of penetration is to retrieve it from classical molecular dynamics simulations, as there is a one-to-one relation between free energies and density profiles. [30] If the activity coefficient is independent of the density, the free energy can be obtained by using the following equation:

$$G(s) = -RT\ln \frac{\rho(s_Z)}{\rho(s_0)} \qquad Eq.7$$

, where $\rho(s_0)$ belongs to the bulk phase density and $\rho(s_Z)$ is the mass density at position Z along the membrane normal.

As the height of the free energy barrier gravely affects the transition rate between different states along the CV, the sampling obtained from classical MD simulations can be insufficient. Biased sampling methods modify the height of the free energy barriers by adding a biasing potential ($P(s(V,r))$ to the potential energy ($U(V,r)$) along CV(s). $P(s(V,r)$ is directly related to the free energy along the CV the following way:

$$P(s) = -G(s) \qquad Eq.8$$

In metadynamics and well-tempered metadynamics (WT-MD) the bias potential appears during the simulations as a repulsive Gaussian, centered on the explored points of a CV(s) space, leading the system towards previously not explored configurations. These Gaussians can be called 'hills' and have a preassigned width (σ) and height (ω) and are deposited at every t' time step as the simulation proceeds, where the collective variable has a value of $s(t')$. The difference between the two methods is that in WT-MD the height of the Gaussians are rescaled as the system passes previously explored

configurations along CV(s), which enables the free energy profile to converge to an exact value. [31], [32]

TWO-PHASE MOLECULAR DYNAMICS SIMULATIONS

Coexisting liquid and vapor phases in the vapor-liquid equilibria (VLE) [33], [34] and the supercritical phase [20] can be investigated by performing two-phase (2φ) simulations, where the resulting bimodal distribution of the mass density can be used to obtain critical parameters. In two-phase Molecular Dynamics the VLE is simulated in an NVT ensemble, where the liquid and vapor phases are in the same simulation box separated by an interface. The great advantage of 2φMD is that the time evolution of the phases and the interface is observable throughout the VLE to the supercritical phase. By applying Voronoi Tessellation (VT) on two-phase simulations a set of molecular volumes, the mean molecular volume and the variance of molecular volumes can also be obtained, which can be directly converted to density distribution of the simulated systems. [24], [33], [34] To separate the molecules of the different phases in the VLE – vapor, liquid and phase transferring molecules – a new method was developed. [24]

In this method Voronoi polygons are created for the center of mass (COM) of each molecule. The distance of the COM and Voronoi vertex i (r_i) is calculated for each vertex in the simulation box. In the case of liquid phase molecules higher sphericity and smaller r_i values are expected, while vapor phase molecules tend to have larger, irregular polygons with low sphericity. 'Phase transferring' molecules can be found at the interface, thus their Voronoi polygons are expected to have irregular shapes also, while on one of their sides they have to have similar properties to the molecules in the liquid phase.

To identify the phase that a molecule belongs to, the maximum value of r_i, noted as $r_{max,liq}$, can be calculated from the 1φMD liquid phase simulations. According to my initial proposition, each liquid phase molecule has to fit into a sphere with a radius equal to $r_{max,liq}$, while vapor phase and phase transferring molecules cannot meet this requirement. In 2φMD simulations each Voronoi cell has a k amount of Voronoi vertices which are closer or in equal distance to the COM of the corresponding molecules than $r_{max,liq}$. Taking the two extremes, the molecule is surely in liquid phase if $k/i = 1$, while in vapor phase if $k/i = 0$, where i is the total amount of Voronoi vertices belonging to a Voronoi cell. Considering instantaneous structural disturbances, wider interval for k/i ratio is required for the proper sorting, therefore an empirical interval parameter, α, has been introduced and its value is chosen to be 0.1. So, if $k/i < \alpha$, a molecule is considered as gas phase; while if $k/i > 1-\alpha$ it is a liquid phase; and if $\alpha \leq k/i \leq 1-\alpha$ it is a 'phase transferring' molecule.

NEW SCIENTIFIC RESULTS – THESIS

Based on the research carried out during my PhD studies the following main conclusions were drawn as new scientific results:

1. The free energy of membrane permeation profiles of the investigated compounds can be classified into three groups with one, two or three free energy barriers being present at the bilayer center, at the site of the headgroups and both in the center and at the headgroups site respectively.

The membrane permeation of eight industrially relevant compounds (1,4-dioxane, phenol, oxane, morpholine, 3-ethylidene-6-vinyltetrahydro-2H-pyran-2-one (EVL), octa-1,3,7-triene (BDDI), 2-vinylhepta-4,6-dienoic acid (AC1), 3-ethylidene-2-methylene-5-(prop-1-en-1-yl)-dihydrofuran (LAC2)) into DPPC composed bilayers were investigated via Well-Tempered Metadynamics. Based on the profiles three different types can be specified: with one free energy barrier - in the cases of AC1 and phenol - which is found in the bilayer center (**Figure 2, Panel A**); with two free energy barriers - in the cases of oxane and BDDI – which is found at the headgroups region (**Figure 2, Panel B**); and with three free energy barriers, in the cases of EVL, 1,4-dioxane, morpholine and LAC2, where the barriers are found at the headgroups region and in the bilayer center (**Figure 2, Panel C**).

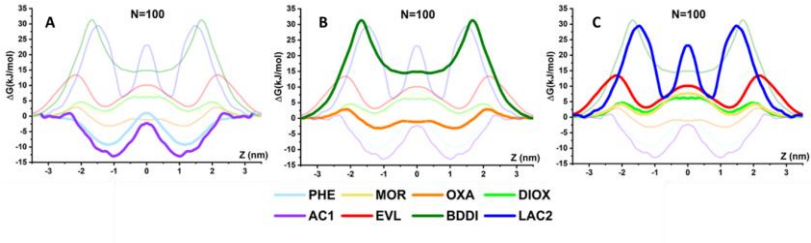

Figure 2 The three different types of membrane permeation profiles. Panel A: Free energy profiles with one free energy barrier; Panel B: Free energy profiles with two free energy barriers; Panel C: Free energy profiles with three free energy barriers

2. The free energy of membrane permeation profile of the investigated compounds show concentration dependence.

The concentration dependence of the membrane permeation of six industrially relevant compounds (1,4-dioxane, phenol, 3-ethylidene-6-vinyltetrahydro-2H-pyran-2-one (EVL), octa-1,3,7-triene (BDDI), 2-vinylhepta-4,6-dienoic acid (AC1), 3-ethylidene-2-methylene-5-(prop-1-en-1-yl)-dihydrofuran (LAC2)) into DPPC composed bilayers were investigated by using Metadynamics and Well-Tempered Metadynamics. In all the cases it was found that the permeation profiles are affected by the permeant concentration. When – due to the limited solubility of the permeant – a liquid droplet is formed in the bulk phase, the free energy barrier increases at a higher concentration; at

the same time in the cases of highly soluble and miscible compounds the free energy barrier in the bilayer center decreases at higher concentration (**Figure 3**).

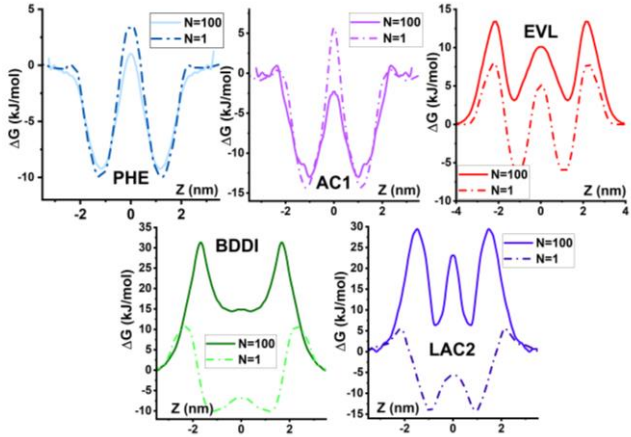

Figure 3 Concentration dependence of the free energy barriers of permeation in the cases of phenol, AC1, EVL, BDDI and LAC2.

3. Density based free energy of membrane permeation calculations can be a reasonable alternative to enhanced sampling methods.

The membrane permeation of eight industrially relevant compounds (1,4-dioxane, phenol, oxane, morpholine, 3-ethylidene-6-vinyltetrahydro-2H-pyran-2-one (EVL), octa-1,3,7-triene (BDDI), 2-vinylhepta-4,6-dienoic acid (AC1), 3-ethylidene-2-methylene-5-(prop-1-en-1-yl)-dihydrofuran (LAC2)) into DPPC composed bilayers were investigated via Well-Tempered Metadynamics and a density based approach (D2E). In this method the free energy profile is obtained based on the density distribution of the investigated compounds in the simulation box along the membrane normal. In almost all cases the permeation profile obtained by WT-MD and D2E were within the limits of chemical accuracy, except in the case of LAC2, where the maximum deviation was 5.4 kJ/mol (**Figure 4**). Based on these results the application of density based free energy of permeation calculations could be a reasonable alternative – or first guess – in the cases of small, neutral molecules.

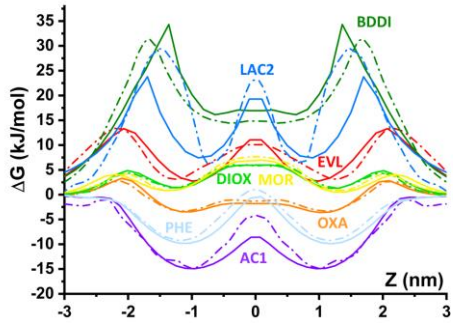

Figure 4 Comparison of the free energy of permeation profiles obtained from D2E and WT-MD methods.

4. The presence of additives can affect the free energy of membrane permeation profile of water molecules, which results in the elevated amount (five times) of water molecules in the bilayer center.

In the cases of 1,4-dioxane, phenol, oxane and morpholine the free energy of membrane permeation of water molecules into DPPC composed model membranes was calculated by using Well-Tempered Metadynamics. It was found that water molecules have a lower permeation barrier when the membrane structure is altered due to the presence of additives. Parallel to the lower free energy barrier, a significantly higher amount of water molecules was found inside the bilayer, which in the presence of oxane – which have a thermodynamically favored position in the bilayer center – exceeded 5 times the amount of molecules compared to the additive free DPPC membranes (**Figure 5**).

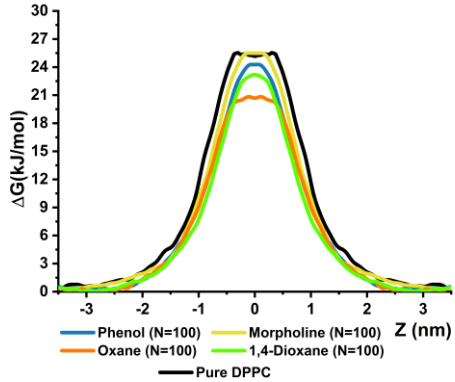

Figure 5 Free energy profiles obtained by WT-MD of a single water molecule penetrating inside DPPC membranes in either clear environment (black), or in the presence of 100 NSO-HET molecules: phenol (blue), morpholine (yellow) or oxane (orange).

5. Based on the free energy profiles and membrane/bulk partition coefficients, a permeation order of the molecules can be established.

The membrane/bulk phase partition coefficient and membrane volume fraction was calculated for 1,4-dioxane, phenol, oxane, morpholine, 3-ethylidene-6-vinyltetrahydro-2H-pyran-2-one (EVL), octa-1,3,7-triene (BDDI), 2-vinylhepta-4,6-dienoic acid (AC1), 2-ethylidenehepta-4,6-dienoic acid (AC2), 3-ethylidene-2-methylene-5-(prop-1-en-1-yl)-dihydrofuran (LAC2), 3-ethyl-5-propylidenefuran-2-one (LAC3) from classical molecular dynamics simulations. Based on these parameters and the free energy profiles, a permeation order of the molecules can be established. In this order three different types of molecules were separated from each other: molecules which do not permeate into the membrane due to their high free energy barriers and low partition coefficient (BDDI, LAC2 and LAC3); molecules which are able to permeate the bilayer, have moderate permeation barriers and slightly negative partition coefficients (EVL, 1,4-dioxane and morpholine); and molecules which can spontaneously diffuse into the bilayer without a free energy barrier, and have positive partition coefficients (phenol, oxane, AC1 and AC2). Based on Mullins's volume fraction theory [8] aside from BDDI, all molecules act as a narcotic in the used simulation environment (**Figure 6**).

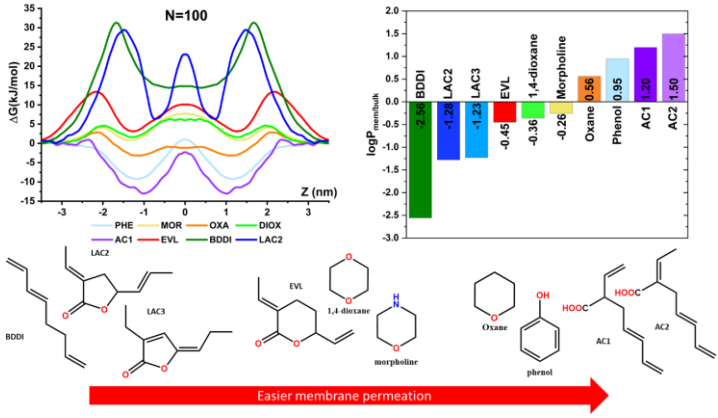

Figure 6 Comparison of free energy profiles and log$P_{mem/bulk}$ values of the investigated molecules, where $N_{compound}$=100. Based on these data a permeation order of the molecules is set, which is indicated by the 2D graph models of the compounds.

6. Vapor, Liquid and Phase transferring molecules were separated from each other based on sphericity in the case of 1,3-butadiene in the Vapor-Liquid Equilibria. By using this method experimentally available densities in the VLE and the supercritical point was reproduced within 10% of deviation.

I have developed a new method for classifying molecules in the vapor-liquid equilibria, which are either in vapor or liquid phase or 'phase transferring'. The method is based on the sphericity of the Voronoi polygons generated for each molecule in a slab simulation. The method was applied in the case of 1,3-butadiene, in the temperature range of 278-408 K, and the experimentally available densities were reproduced within 5 kg/m^3. On the computed dataset the law of rectilinear diameters and the Wegner equation was applied and the supercritical temperature and density were obtained within 10% of deviation (**Figure 7**).

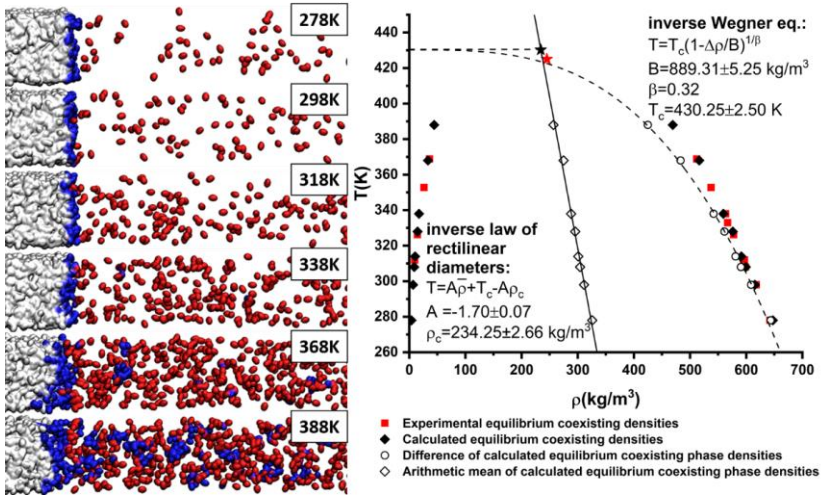

Figure 7 Molecular and density distribution of the coexisting phases in the VLE. In the molecular distribution white indicates the liquid and red the vapor phase molecules, while blue highlights the 'phase transferring' molecules

7. The temperature dependence of Specific Surface Area in the Vapor-Liquid Equilibria can be used to obtain the supercritical temperature.

The temperature dependence of Specific Surface Area (SSA) in the Vapor-Liquid Equilibria was investigated in the case of 1,3-butadiene, and it was found that an empirical equation can be fitted on this diagram:

$$SSA(T) = aT - b \times \arctan\big(c(T_c - T)\big)$$

From this $T_{c,SSA}$ = 426.50 K was obtained, which is within 1% of deviation from the experimental value of the supercritical temperature (**Figure 8**). At the same time the theoretical limit of the total molecular surface of the system can be obtained by

assuming that none of the 1,3-butadiene molecules have any contact with the others; which results in the value of SSA as large as 24944 m^2/g for 1,3-butadiene. At the critical point, the SSA_{Tc} is 10660.26 m^2/g which is 42.74% of the maximum value, while it goes up to 77.71% at 510 K (SSA_{510K} = 19383 m^2/g).

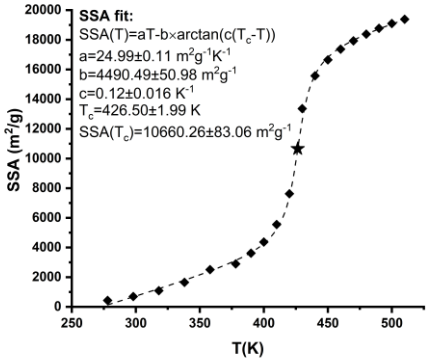

Figure 8 Temperature dependence of Specific Surface Area of 1,3-butadiene in sub and supercritical conditions. The investigated temperature interval was 278-510 K. The values of SSA are obtained from NPT liquid and supercritical simulations. The SSA values are indicated with black diamonds, and the supercritical point is indicated with a black star.

SUMMARY

The chemical industry produces a grave amount of substances annually, out of which a non-negligible portion is released into the environment, leading to ascendant environmental stress. At the same time the health and environmental effects of most chemicals is yet to be understood. For the support of environmental and toxicological sciences, the effect and structure of chemically inert industrial compounds can be characterized by using the tools of computational chemistry.

Throughout my work the passive membrane permeation of 10 industrially relevant compounds were investigated by the means of molecular dynamics. In all of the investigated cases it was found that the compounds can permeate inside DPPC composed model biological membranes, and promote changes in the bilayer structure. Aside from the structural changes the free energy of permeation of the different compounds were investigated and it was found that this process is highly dependent on concentration. Also the permeation of additives can decrease the permeation barrier of water molecules too. Based on the volume fraction theory aside from BDDI, all molecules act as a narcotic in the set simulation environment. The general methodology described in this doctoral dissertation could be applied in the future for several other compounds to get a better understanding on the molecular process of the interactions of additives with biological membranes.

The vapor-liquid equilibria and supercritical phase of 1,3-butadiene was described at by using two-phase molecular dynamics. To be able to accurately predict the vapor and liquid densities of 1,3-butadiene from the slab simulations and to select the phase transferring molecules, I have elaborated a new method, where with a single parameter, the molecules of different phases can be separated based on the sphericity of their Voronoi polygons. By using this method, the vapor and liquid densities of the VLE-curve and supercritical point of 1,3-butadiene were reproduced within 10 % compared to experimental values By pairing the used methods and model with an appropriate CO_2 force field, their two-component system could be investigated in detail at different compositions and environment, in order to understand the reaction, and fine-tune it towards higher EVL selectivity.

ÖSSZEFOGALÁS

A vegyipar éves szinten több, mint 10^8 tonna vegyi anyagot állít elő. Ennek nem elhanyagolható része kerül a környezetbe kezeletlenül, ami egyre növekvő környezeti stresszhez vezet, miközben a legtöbb vegyi anyag egészségügyi és környezeti kockázatát még nem ismerjük. A környezettudományok és a toxikológia támogatása érdekében az inert ipari vegyületek hatását és szerkezetét a számításos kémia eszközeivel jól jellemezhetjük.

Munkám során 10, ipari szempontból releváns vegyület passzív membránpermeációját vizsgáltam molekuladinamikai módszerekkel. Valamennyi vizsgált esetben megállapítható, hogy a vegyületek képesek a DPPC összetételű biológiai modellmembránok belsejébe hatolni, ahol elősegítik a kettősréteg szerkezetének megváltozását. A szerkezeti változások mellett a különböző vegyületek permeációs szabadenergiáját is vizsgáltam, amelyből megállapítható, hogy ez a folyamat nagymértékben koncentrációfüggő. Emellett az adalékanyagok permeációja csökkeni a vízmolekulák permeációs gátját is. A térfogatarány-elmélet alapján a BDDI-n kívül minden molekula narkotikumként viselkedik a beállított szimulációs környezetben. A doktori disszertációmban leírt általános módszertan a jövőben számos más vegyületre is alkalmazható lehet annak érdekében, hogy jobban megértsük az kemikáliák biológiai membránokkal való kölcsönhatásának molekuláris folyamatát.

Az 1,3-butadién gőz-folyadék egyensúlyát (VLE) és szuperkritikus fázisát kétfázisú molekuladinamikával vizsgáltam. Annak érdekében, hogy a kétfázisú szimulációk alapján az 1,3-butadién gőz- és folyadéksűrűségét pontosan megállapíthassam és a fázist váltó molekulákat kiválaszthassam, egy új módszert dolgoztam ki. Ennek a módszernek az alkalmazásával egyetlen paraméterrel elkülöníthetővé válnak a különböző fázisok molekulái a hozzájuk tartózó Voronoi-poligonok gömbszerűsége alapján. A módszert felhasználva a VLE-görbe és a szuperkritikus pont kísérleti értékei 10 %-os egyezést mutattak az 1,3-butadién esetén. Ha az alkalmazott módszereket és butadién modellt megfelelő CO_2 erőtérrel párosítjuk a későbbiekben, akkor a két komponensű rendszerük részletesen vizsgálható lesz különböző összetételek és környezeti paraméterek mellett. Ezáltal lehetővé válik a reakció megértése és a reakció finomhangolása a nagyobb EVL-szelektivitás érdekében.

REFERENCES

[1] Z. Wang, G. W. Walker, D. C. G. Muir, and K. Nagatani-Yoshida, "Toward a Global Understanding of Chemical Pollution: A First Comprehensive Analysis of National and Regional Chemical Inventories," *Environ. Sci. Technol.*, vol. 54, no. 5, pp. 2575–2584, 2020.

[2] R. A. Sheldon, "The E Factor: Fifteen years on," *Green Chem.*, vol. 9, no. 12, pp. 1273–1283, Nov. 2007.

[3] M. L. Diamond *et al.*, "Exploring the planetary boundary for chemical pollution," *Environ. Int.*, vol. 78, pp. 8–15, 2015.

[4] S. Seethapathy, T. Górecki, and X. Li, "Passive sampling in environmental analysis," *J. Chromatogr. A*, vol. 1184, no. 1–2, pp. 234–253, 2008.

[5] D. Mackay, J. A. Arnot, E. P. Petkova, and K. B. Wallace, "The physicochemical basis of QSARs for baseline toxicity," *SAR QSAR Environ. Res.*, vol. 20, no. 3–4, pp. 393–414, 2009.

[6] M. Nendza, M. Müller, and A. Wenzel, "Discriminating toxicant classes by mode of action: 4. Baseline and excess toxicity," *SAR QSAR Environ. Res.*, vol. 25, no. 5, pp. 393–405, 2014.

[7] J. J. Li *et al.*, "Development of thresholds of excess toxicity for environmental species and their application to identification of modes of acute toxic action," *Sci. Total Environ.*, vol. 616–617, pp. 491–499, 2018.

[8] J. L. Mullins, "Some physical mechanisms in narcosis," *Chem. Rev.*, vol. 54, no. 2, pp. 289–323, 1954.

[9] D. Van Der Spoel, S. Manzetti, H. Zhang, and A. Klamt, "Prediction of Partition Coefficients of Environmental Toxins Using Computational Chemistry Methods," *ACS Omega*, vol. 4, no. 9, pp. 13772–13781, 2019.

[10] A. Krämer *et al.*, "Membrane permeability of small molecules from unbiased molecular dynamics simulations," *J. Chem. Phys.*, vol. 153, no. 12, p. 124107, 2020.

[11] J. Sikkema, J. A. de Bont, and B. Poolman, "Mechanisms of membrane toxicity of hydrocarbons.," *Microbiol. Rev.*, vol. 59, no. 2, pp. 201–22, Jun. 1995.

[12] M. S. I. Shaikh, N. D. Derle, and R. Bhamber, "Permeability enhancement techniques for poorly permeable drugs: A review," *J. Appl. Pharm. Sci.*, vol. 2, no. 7, pp. 34–39, 2012.

[13] S. Peddinghaus *et al.*, "Quantitative assessment of the embryotoxic potential of NSO-heterocyclic compounds using zebrafish (Danio rerio)," *Reprod. Toxicol.*, vol. 33, no. 2, pp. 224–232, 2012.

[14] M. Brinkmann *et al.*, "Ecotoxicity of Nitrogen, Sulfur, or Oxygen Heterocycles and Short-Chained Alkyl Phenols Commonly Detected in Contaminated Groundwater," *Environ. Toxicol. Chem.*, vol. 38, no. 6, pp. 1343–1355, 2019.

[15] P. Braunstein, D. Matt, and D. Nobel, "Carbon Dioxide Activation and Catalytic Lactone Synthesis by Telomerization of Butadiene and CO2," *J. Am. Chem. Soc.*, vol. 110, no. 10, pp. 3207–3212, 1988.

[16] L. Chen, J. Ling, X. Ni, and Z. Shen, "Synthesis and Properties of Networks Based on Thiol-ene Chemistry Using a CO2-Based δ-Lactone," *Macromol. Rapid Commun.*, vol. 39, no. 23, pp. 1–6, 2018.

[17] X. L. L. He, "Synthesis of Lactones and Other Heterocycles," *Top. Curr. Chem.*, vol. 375, no. 2, pp. 1–32, 2017.

[18] T. Adschiri and A. Yoko, "Supercriticalfluids for nanotechnology," *J. Supercrit. Fluids*, vol. 134, pp. 167–175, 2018.

[19] M. Türk and C. Erkey, "Synthesis of supported nanoparticles in supercritical fluids by supercritical fl uid reactive deposition: Current state, further perspectives and needs," *J. Supercrit. Fluids*, vol. 134, pp. 176–183, 2018.

[20] J. M. Stubbs, "Molecular simulations of supercritical fluid systems," *J. Supercrit. Fluids*, vol. 108, pp. 104–122, 2016.

[21] Z. B. Rózsa, L. J. Németh, B. Jójárt, K. Nehéz, B. Viskolcz, and M. Szőri, "Molecular Dynamics and Metadynamics Insights of 1,4-Dioxane-Induced Structural Changes of Biomembrane Models," *J. Phys. Chem. B*, vol. 123, no. 37, pp. 7869–7884, 2019.

[22] Z. B. Rózsa, E. Szőri-Dorogházi, B. Viskolcz, and M. Szőri, "Transmembrane penetration mechanism of cyclic pollutants inspected by molecular dynamics and metadynamics: the case of morpholine, phenol, 1,4-dioxane and oxane," *Phys. Chem. Chem. Phys.*, vol. 23, pp. 15338–15351, 2021.

[23] Z. B. Rózsa, R. Thangaraj, B. Viskolcz, and M. Szőri, "Foreseeing the future of green Technology. Molecular dynamic investigation on passive membrane penetration by the products of the CO2 and 1,3-butadiene reaction," *J. Mol. Liq.*, vol. 361, p. 119581, Sep. 2022.

[24] Z. B. Rózsa, B. Minofar, D. Řeha, B. Viskolcz, and M. Szőri, "From the vapor-liquid equilibrium to the supercritical condition. Molecular dynamics modeling of 1,3-butadiene," *J. Mol. Liq.*, 2020.

[25] G. Raabe, *Applications and Perspectives Molecular Simulation Studies on Thermophysical Properties With Application to Working Fluids*. Braunschweig: Springer, 2017.

[26] J. M. Berg, J. L. Tymoczko, and L. Stryer, *Biochemisty, 5th edition*, 5th editio. New York: NCBI, 2002.

[27] A. L. Parrill and K. B. Lipkowitz, *Reviews in Computational Chemistry 28*. New Jersey: John Wiley & Sons, 2015.

[28] T. Steinbrecher, R. Abel, A. Clark, and R. Friesner, "Free Energy Perturbation Calculations of the

Thermodynamics of Protein Side-Chain Mutations," *J. Mol. Biol.*, vol. 429, no. 7, pp. 923–929, 2017.
[29] J. Vymetal and J. Vondrásek, "Metadynamics As a Tool for Mapping the Conformational and Free-Energy Space of Peptides - The Alanine Dipeptide Case Study," *J. Phys. Chem. B*, vol. 114, no. 16, pp. 5632–5642, 2010.
[30] A. Arslanargin and T. L. Beck, "Free energy partitioning analysis of the driving forces that determine ion density profiles near the water liquid-vapor interface," *J. Chem. Phys.*, vol. 136, no. 10, p. 104503, 2012.
[31] D. Meral, D. Provasi, and M. Filizola, "An efficient strategy to estimate thermodynamics and kinetics of G protein-coupled receptor activation using metadynamics and maximum caliber," *J. Chem. Phys.*, vol. 149, no. 22, p. 224101, 2018.
[32] A. Barducci, G. Bussi, and M. Parrinello, "Well-Tempered Metadynamics: A Smoothly Converging and Tunable Free-Energy Method," *Phys. Rev. Lett.*, vol. 100, no. 2, p. 020603, 2008.
[33] J. T. Fern, D. J. Keffer, and W. V. Steele, "Vapor - Liquid equilibrium of ethanol by molecular dynamics simulation and voronoi tessellation," *J. Phys. Chem. B*, vol. 111, no. 46, pp. 13278–13286, 2007.
[34] S. Patel, W. V. Wilding, and R. L. Rowley, "The use of two-phase molecular dynamics simulations to determine the phase behavior and critical point of propane molecular models," *J. Chem. Phys.*, vol. 134, no. 2, 2011.

LIST OF PUBLICATIONS

Publications related to the subject of the dissertation:

1. Rózsa, Zsófia Borbála; Németh, Lukács József; Jójárt, Balázs; Nehéz, Károly; Viskolcz, Béla; Szőri, Milán
Molecular Dynamics and Metadynamics Insights of 1,4-Dioxane-Induced Structural Changes of Biomembrane Models
JOURNAL OF PHYSICAL CHEMISTRY B: 123, 7869-7884 (2019)
Q1, IF: 2.857, Independent citations: 2

2. Rózsa, Zsófia Borbála; Minofar, Babak; Řeha, David; Viskolcz, Béla; Szőri, Milán
From the vapor-liquid equilibrium to the supercritical condition. Molecular dynamics modeling of 1,3-butadiene
JOURNAL OF MOLECULAR LIQUIDS: 315, 113702 (2020)
Q1, IF: 5.85, Independent citations: 2

3. Rózsa, Zsófia Borbála; Szőri-Dorogházi, Emma; Viskolcz, Béla; Szőri, Milán
Transmembrane penetration mechanism of cyclic pollutants inspected by molecular dynamics and metadynamics: the case of morpholine, phenol, 1,4-dioxane and oxane
PHYSICAL CHEMISTRY CHEMICAL PHYSICS: 28. 15338-15351. (2021)
IF: 3.603, Q1

4. Rózsa Zsófia Borbála; Thangaraj Ravikumar; Viskolcz Béla; Szőri Milán
Foreseeing the future of green Technology. Molecular dynamic investigation on passive membrane penetration by the products of the CO_2 and 1,3-butadiene reaction
JOURNAL OF MOLECULAR LIQUIDS: 361, 119581. (2022)
IF: 6.165, Q1

Further publications

1. Cheikh, Wafaa ; **Rózsa, Zsófia Borbála**; Camacho López, Christian Orlando; Mizsey, Péter; Viskolcz, Béla; Szőri, Milán; Fejes, Zsolt
Urethane Formation with an Excess of Isocyanate or Alcohol: Experimental and Ab Initio Study
POLYMERS 11, 1543 (2019)
Q1, IF: 3.426, Independent citations: 9

2. Illés, Ádám; **Rózsa, Zsófia Borbála**; Thangaraj, Ravikumar; Décsiné Gombos, Erzsébet; Dóbé, Sándor; Giri, Binod Raj; Szőri, Milán
An experimental and theoretical kinetic study of the reactions of hydroxyl radicals with tetrahydrofuran and two deuterated tetrahydrofurans
CHEMICAL PHYSICS LETTERS 776, 138698 (2021)
Q2, IF: 2.58, Independent citations: 1

Presentations related to the dissertation

1. 8th Visegrad Symposium on Structural Systems Biology (Losonc, Slovakia) 2018
Dioxane-induced changes on the interfacial region of phosphatidyl-choline membranes
2. KeMoMo-QSAR Szimpózium (Szeged, Hungary) 2019
Az 1,3-butadién strukturális változásainak megértése molekuláris szinten a gőz-folyadék egyensúlytól a szuperkritikus állapotig
3. Eötvös-Symposium (Miskolc, Hungary) 2019
Molecular Understanding of Structural Changes of 1,3-Butadiene from Vapor-Liquid Equilibrium to Supercritical Conditions
4. 9th Visegrad Symposium on Structural Systems Biology (Szilvásvárad, Hungary) 2019
Molecular Dynamics and Metadynamics Insights of 1,4-Dioxane Induced Structural Changes of Biomembrane Models
5. 10th Visegrad Symposium on Structural Systems Biology (Nové Hrady, Czech Republic) 2022
Molecular-level understanding of membrane permeation of some chemicals

Further Presentations

1. 5th Visegrad Symposium on Structural Systems Biology (Szeged, Magyarország) 2015
Mapping out the 366 shades of the $C_4H_8O_2$ isomers
2. Annual Summer School in Molecular Biophysics and Systems Biology (Nové Hrady, Czech Republic) 2018

The effect of fatty acids on the conformation of protein channel TRAAK

Posters related to the dissertation

1. 7th Visegrad Symposium on Structural Systems Biology (Nové Hrady, Czech Republic) 2017
A molecular dynamics study on the effects of 1,4-dioxane on model membranes

Further posters

1. 4th Visegrad Symposium on Structural Systems Biology (Nové Hrady, Czech Republic) 2014
A theoretical analysis on the thermodynamic stability of various constitutional isomers of $C_4H_8O_2$

Scientometrics

- Total number of publications: 6
- Total number of first author publications: 4
- Total number of Q1 publications: 5
- Total number of Q2 publications: 1
- Total number of independent citations: 14
- H index: 3